Domains I and III of the Human Copper Chaperone for Superoxide Dismutase Interact via a Cysteine-Bridged Dicopper(I) Cluster†

John F. Eisses,‡ Jay P. Stasser,§ Martina Ralle,§ Jack H. Kaplan,*,‡ and Ninian J. Blackburn*,§

Department of Biochemistry and Molecular Biology, Oregon Health Sciences University, Portland, Oregon 97201, and Department of Biochemistry and Molecular Biology, Oregon Graduate Institute of Science and Technology, Beaverton, Oregon 97006-8921

Received March 27, 2000; Revised Manuscript Received May 1, 2000

ABSTRACT: Copper binding to the human copper chaperone for superoxide dismutase (hCCS) has been investigated by X-ray absorption spectroscopy. Stoichiometry measurements on the dialyzed, as-isolated protein indicated that up to 3.5 Cu ions bound per hCCS molecule. Reduction with either sodium dithionite or dithiothreitol decreased the copper binding ratio to 2 coppers per hCCS monomer. Analysis of the as-isolated EXAFS data indicated coordination of Cu by a mixture of S and N backscatterers, suggestive of heterogeneous binding of copper between Cu−cysteine binding sites of domain I or III and copper−histidine SOD1-like metal binding sites of domain II. The best fit was obtained with 1.6 Cu−S (cysteine) at 2.24 Å ($2\sigma^2 = 0.011$ Å^2) and 1.1 N (histidine) at 1.98 Å ($2\sigma^2 = 0.005$ Å^2). A peak of variable intensity in the Fourier transform (FT) of the as-isolated protein at 2.7 Å was suggestive of the presence of a heavy atom scatterer such as Cu. Analysis of the dithionite- and DTT-reduced derivatives indicated that copper was lost from the histidine coordinating sites, resulting in a S-only environment with copper coordinated to three S backscatterers at 2.26 Å. The heavy atom scatterer peak was now prominent in the FT and could be well fit by a Cu−Cu interaction at 2.72 Å. The data were best interpreted by a dinuclear μ_2-bridged cluster with doubly bridging cysteine ligands similar to the cluster proposed to exist in the cytochrome *c* oxidase chaperone COX17. Analysis of primary sequence and X-ray structural information on yeast CCS strongly suggests that this cluster bridges between domains I and III in hCCS. A mechanism for copper translocation is briefly discussed.

SOD1 (the Cu, Zn superoxide dismutase) is a homodimeric enzyme (32 kDa) whose major function is thought to be the catalytic conversion of superoxide radicals to hydrogen peroxide and oxygen (*1*, *2*). This reaction is dependent on an active site containing the metal ions Cu and Zn (*3*−*5*). Many studies have shown a connection between SOD1 and familial amylotrophic lateral sclerosis (for example, see refs *6*−*8*). This connection may be due to mutations that foster aberrant copper chemistry at the SOD1 active site leading to increased production of harmful free radicals such as hydroxyl and peroxynitrite (*9*−*12*). SOD1 acquires its copper through a direct interaction with its copper chaperone, CCS[1] (*13*−*15*), and recent evidence suggests that SOD1 is incapable of acquiring Cu ions in the absence of the CCS protein (*13*). CCS is composed of a three-domain structure. Domain 1 (residues 1−85) contains a MTCXXC motif conserved in a number of other metal chaperones and in the N-terminal subdomains of Menkes and Wilson proteins; it is thought to be a locus of Cu binding (*12*, *16*−*20*). Domain 2 (residues 86−234) has sequence homology to the SOD1 monomer and in particular to residues associated with (i) the Cu and Zn binding residues [but excluding the copper ligand H120 which is an Asp in human CCS (hCCS)] and (ii) the native SOD dimer interface. Domain 3 (residues 235−274) contains a CXC motif which has also been implicated in metal translocation (*21*). X-ray crystal structures of yeast CCS (yCCS)[1] have recently been reported and demonstrate the expected structural homology between domain I and Atx1 and between domain II and SOD1 (*22*). Unfortunately, the structures were uninformative with respect to copper binding, since the putative metal binding cysteine residues in domain I were oxidized in a disulfide and domain III was disordered. A recent study (*15*) has demonstrated complex formation between CCS and SOD1, but the domains that interact in the formation of the CCS/SOD1 complex are unknown. Here we report the results of an X-ray absorption spectroscopy (XAS) structural investigation of the copper binding to hCCS and report the unexpected result that domains I and III appear to interact via a cysteine-bridged dinuclear copper cluster.

† This work was supported by National Institutes of Health Grants GM54803 (N.J.B.) and HL30315 (J.H.K.).

* To whom correspondence should be addressed. N.J.B.: Oregon Graduate Institute of Science and Technology, 20000 NW Walker Road, Beaverton, OR 97006-8921. Phone: (503) 748-1384. Fax: (503) 748-1464. E-mail: ninian@bmb.ogi.edu. J.H.K.: Oregon Health Sciences University, 3181 SW Sam Jackson Park Road, Portland, OR 97201. Phone: (503) 494-1655. Fax: (503) 494-8393. E-mail: kaplanj@ohsu.edu.

‡ Oregon Health Sciences University.

§ Oregon Graduate Institute of Science and Technology.

[1] Abbreviations: CCS, copper chaperone for superoxide dismutase; DTT, dithiothreitol; EPR, electron paramagnetic resonance; EXAFS, extended X-ray absorption fine structure; hCCS, human CCS; XAS, X-ray absorption spectroscopy; yCCS, yeast CCS.

10.1021/bi000690j CCC: $19.00
Published on Web 05/31/2000

Table 1: Copper Binding Properties of hCCS

	sample	protein (P) (μM)	Cu_{total} (μM)	Cu/P	Cu(I) (μM)	Cu(I)/P	Cu(II) (μM)	Cu(II)/P
A	undialyzed	776	1500	1.9				
B	undialyzed	867	1677	1.9				
C	first dialysis	67	227	3.4				
	second dialysis	48	152	3.2	92	1.9	60	1.3
	+1 mM DTT	12	26	2.2	26	2.2	0	0
D	undialyzed	41	100	2.5				
	dialyzed	39	97	2.5				
	concd for XAS	275	669	2.4	494	1.8	175	0.6
	+1 mM dithionite	78	156	2.0	156	2.0	0	0
	+1 mM DTT	75	158	2.1	158	2.1	0	0

EXPERIMENTAL PROCEDURES

Cloning, Expression, and Purification. hCCS cDNA was cloned into the pMAL-c2X expression vector (New England Biolabs). The protein was expressed in *Escherichia coli* strain BL21(DE3) after induction with IPTG. The maltose binding protein−CCS fusion was purified over an amylose resin column following the manufacturer's guidelines. The copper content of the expressed protein was determined by the bicinchoninic acid-based assay (Sigma) and by atomic absorption spectrophotometry.

Samples for XAS were concentrated in an Amicon centricon ultrafiltration cell. In some cases, samples were dialyzed versus 50 mM potassium phosphate, pH 7.5, to remove adventitiously bound copper ions. Dithionite- or dithiothreitol-reduced samples were prepared by adding a 10 μL aliquot of a stock solution of reductant prepared fresh each time, followed by one additional dialysis step against 50 mM potassium phosphate, pH 7.5. The final concentration of reductant prior to dialysis was 20 mM for sample B and 1 mM for samples D (Table 1).

XAS Data Collection and Analysis. Cu K-edge (8.979 keV) extended X-ray absorption fine structure (EXAFS) and X-ray absorption near-edge structure data for hCCS were collected at the Stanford Synchrotron Radiation Laboratory (40−100 mA, 3 GeV). Samples A and B (Table 1) were measured on BL 7-3 (Si[220], detuned 50% to reject harmonics), whereas samples D were measured on BL 9-3 (Si[220], Rh-coated mirror upstream of the monochromator to reject harmonics, no detuning) in fluorescence mode using a high-count-rate Canberra 13-element (BL 7-3) or 30-element (BL 9-3) Ge array detector with maximum count rates below 120 kHz. A 6 μm Ni filter and Soller slit assembly were placed in front of the 30-element detector on BL 9-3 to reduce the elastic scatter peak. For data collected on BL 9-3 (samples D), nine scans of a sample containing only sample buffer were averaged and subtracted from the averaged data for the protein samples. This procedure removed the small amount of residual Ni Kβ fluorescence from the Ni filter as well as a minor contamination from a copper metal impurity in the cryostat windows, allowing data of excellent signal-to-noise ratio to be collected down to 100 μM total copper in the sample. The samples (70 μL) were measured as aqueous glasses (>20% ethylene glycol) at 15 K. Energy calibration was achieved by reference to the first inflection point of a copper foil (8980.3 eV), which was simultaneously measured. Data reduction and background subtraction were performed using the program modules of EXAFSPAK (*23*). Data from each detector channel were inspected for glitches or drop outs before being included in the final average. Spectral simulation was carried out using the program EXCURV98 (*24*−*27*) and the OPT module in EXAFSPAK with theoretical phase shifts and amplitude functions calculated by FEFF 7.0 (*28*). Both programs gave equivalent results.

RESULTS AND DISCUSSION

Copper Binding to hCCS. The stoichiometry of copper binding to hCCS was examined and compared with that recently reported for the yeast protein (*21*). The results are shown in Table 1. The Cu/protein ratio for native hCCS as isolated was found to vary between 1.9 and 3.4. Preparations were dialyzed versus 50 mM potassium phosphate buffer to determine how much of the copper was adventitiously bound to the protein. In general, dialysis did not reduce the ratio significantly, suggesting that hCCS may contain up to four copper binding sites per monomer. For example, in one experiment (C, Table 1), hCCS as isolated contained 3.4 coppers per protein. After two cycles of dialysis against 50 mM potassium phosphate, the Cu/protein ratio fell to 3.2. Of this, 38% was Cu(II) and 61% was Cu(I) [or spin coupled Cu(II)] as determined by EPR, equating to 1.3 mole equiv of Cu(II) and 1.9 mole equiv of EPR nondetectable copper per protein. Reduction with either sodium dithionite or dithiothreitol, followed by dialysis versus 50 mM potassium phosphate, reduced the Cu/protein ratio to 2.2, all of which was now EPR nondetectable, presumably Cu(I). These results show that reduction caused loss of an amount of copper approximately equivalent to the total Cu(II) component in the original sample. Similar results (Table 1) were obtained when samples with different starting copper concentrations were subjected to the same procedures. Therefore, hCCS appears to contain a heterogeneous population of copper sites in excess of 3 Cu ions per protein in an aerobic environment but approaches a ratio of 2 coppers per protein under reducing conditions.

Schmidt et al. (*21*), investigating copper binding to the yeast protein, found that yCCS bound a maximum of 2 coppers per protein molecule. By comparing the activity of the native chaperone with truncation mutants which lacked either domain I or domain III, these workers were able to show that only domain III was critical for yCCS activity. The domain II/III truncation mutant exhibited low levels of SOD1 activation at low levels of intracellular copper but was markedly stimulated by either the addition of isolated domain I or nontoxic levels of added copper. These results suggested that domain III contained a copper site essential for the CCS−SOD1 transmetalation reaction, while domain I was important in scavenging copper from the cell or accepting the metal from the membrane-bound copper transporters. Mutagenesis was used to show that a CXC sequence in domain III was almost certainly the site of SOD1 transmetalation activity, while the MTCXXC motif in domain I was likely the other copper binding site. In addition, it was shown that the secretory pathway chaperone Atx1 could not substitute for CCS domain I with respect to this scavenging role, indicating that the MTCXXC motif alone was insufficient to impart function and that other functionality was

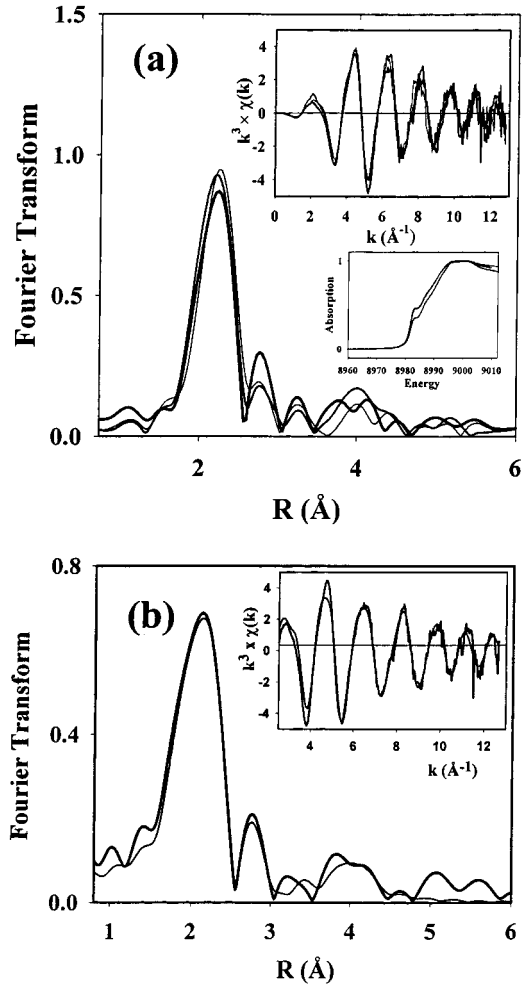

FIGURE 1: (a) Comparison of Fourier transforms, EXAFS (top inset), and absorption edges (bottom insert) for three different preparations of hCCS: thin line, sample A; medium line, sample B; thick line, sample D, concentrated for XAS (Table 1). (b) Experimental (thick line) versus simulated (thin line) Fourier transform and EXAFS (inset) (unfiltered spectra) of hCCS (sample D, concentrated for XAS) (see Table 1). Parameters used in the fits are given in Table 3.

present in domain I, probably related to interdomain interaction.

X-ray crystallography has failed to establish the identity and structure of the copper centers in yCCS, since the pair of cysteines in the MTCXXC motif form a disulfide bond, and domain III is disordered and not observed in the structure (*22*). The overall protein folds of domains I and II are homologous to the Hg(II)−Atx1 (*17*) and Cu/Zn−SOD monomer (*3*), respectively, so that potential copper binding sites can be inferred. This analysis indicates that in yCCS both the zinc binding loop and the catalytic copper site of the SOD-like domain II are absent. Thus, the two copper sites identified from activity studies on the truncation mutants almost certainly arise from the bis-cysteinate MTCXXC and CXC sequences of domains I and III, respectively. However, in hCCS the zinc loop and the catalytic copper site are still present and capable of binding metals, although the residue corresponding to the copper ligand H120 is an aspartate. In fact, Zn binding to the Zn loop of hCCS has recently been confirmed by X-ray crystallography of an isolated domain II fragment, but no metal was bound in the "catalytic" (Cu) site (*29*). Since SOD is known to be capable of binding copper in both of its metal binding sites (*30*), either of these sites is a candidate for the additional cupric copper ions found experimentally in hCCS.

Table 2: Fits Obtained from Analysis of First-Shell Fourier Filtered Data of hCCS[a]

fit no.	shell	distance	$2\sigma^2$ (Å^2)	E_0	F
A	3.10 N	2.07	0.012	−8.90	0.944
B	3.27 S	2.20	0.022	5.05	0.120
C	3.00 S	2.20	0.020	4.89	0.098
D	2.00 S	2.23	0.010	5.16	0.063
	1.00 S	2.10	0.008		
E	1.00 S	2.27	0.007	5.45	0.068
	2.00 S	2.15	0.014		
F	2.00 S	2.22	0.015	1.15	0.054
	1.00 N	1.96	0.009		
G	1.00 S	2.25	0.008	−2.65	0.064
	2.00 N	2.01	0.010		
H	1.36 S	2.24	0.011	−1.01	0.041
	1.47 N	1.99	0.008		

[a] Sample D, concentrated for XAS (R = 1.0−2.2 Å, uncorrected for the phase shift).

X-ray Absorption Spectroscopy. The above copper binding behavior was further investigated by XAS. Figure 1a compares XAS data (FT, EXAFS, and absorption edges) for three different preparations of hCCS, corresponding to samples A, B, and D (D, concentrated for XAS) in Table 1. It is clear that, although the Cu/protein ratio varies among the different samples, the XAS spectra are remarkably similar. The absorption edges of samples A and D are superimposable, while that of sample B is shifted to higher energy, suggestive of a greater level of cupric copper. [The Cu(II)/P ratio of sample B was determined after the XAS experiment and was found to be 30%.] The spectra are dominated by the first-shell peak in the FT but also show weak outer shell interactions. The peak around 4 Å may suggest C_γ/N_γ imidazole outer shell scattering. The position of the peak of variable intensity at ∼2.7 Å is a little too short for imidazole C_β scattering, and interestingly its intensity appears to correlate with the Cu/P ratio of the preparations.

The data were further analyzed by curve fitting, initially using first shell Fourier filtered data (transform range 1.0−2.2 Å, uncorrected for the phase shift) and then by single and multiple scattering analysis of the unfiltered data. The results of the first shell analysis are given in Table 2. Simulations which involved only a single shell of scatterers (either S or N/O) gave poorer fits, particularly for N/O as backscatterer. Better fits were obtained for combinations of S and N scatterers or for a 2:1 split S shell, but the analysis did not unambiguously distinguish between these models. Consideration of the derived Cu−S versus Cu−N distances would seem to exclude the split S shell fit. Reference to Cu−S-containing model complexes (Cambridge Crystallographic Data Base) indicates that the two Cu−S interactions at 2.25 Å and one Cu−N (His) at 1.98 Å are typical for three-coordinate Cu(I) with a S_2N ligand donor set (*31*−*33*). However, a Cu−S interaction at 2.15 Å, as suggested for the split S shell in fit E, is unusually short and is found only in cupredoxin (blue copper) centers, where the protein fold maintains an entatic state (*34*−*36*). The best fit was obtained when the S and N coordination numbers were allowed to float, giving values of 1.4 S and 1.5 N.

Table 3: Parameters Used in the Full Least-Squares Simulation of the Unfiltered Background-Subtracted EXAFS Data of hCCS As Isolated,[a] Using Single and Multiple Scattering Contributions

first shell[b]			outer shells[b]			
shell (X)	R (Å)	$2\sigma^2$ (Å^2)	shell (Y)	R (Å)	∠Cu−X−Y (deg)	$2\sigma^2$ (Å^2)
			$F = 0.573$, $E_0 = -3.31$ eV			
1.1 N_α (imid)	1.98	0.005	1.1 C_β (imid)	2.99	128	0.005
			1.1 C_β (imid)	2.97	232	0.005
1.6 S	2.24	0.011	1.1 C_γ/N_γ (imid)	4.13	163	0.012
1.1 Cu	2.74	0.017	1.1 C_γ/N_γ (imid)	4.06	197	0.012

[a] Sample D, concentrated for XAS; see Table 1. [b] Estimated errors in distances are ±0.02 Å for the first shell and ±0.05 Å for outer shells. Estimated errors in coordination numbers are ±25%. ∠Cu−X−Y represents the angle between the first shell scatterer (X) and the outer shell scatterer (Y). Imidazole outer shell distances and angles are constrained to be within 0.2 Å and 5°, respectively, of the idealized geometry for an imidazole ring.

The results of the first shell analysis can be interpreted in two ways. It is possible that the copper centers reside in a homogeneous environment composed of mixed S/N coordination. However, as discussed above, available structural data are more consistent with heterogeneous binding sites, derived from both the domain I and/or domain III cysteine binding motifs and the domain II SOD-like histidine binding sites. To further investigate these possibilities, we performed simulations of the raw unfiltered data using multiple scattering analysis to include imidazole outer shell interactions. The results are shown in Figure 1b and Table 3. The data can be well fit to 2 ± 0.5 S scatterers at 2.24 Å and 1 ± 0.3 N (imidazole) scatterers at 1.98 Å, with the best fit corresponding to coordination numbers of 1.6 and 1.1 for the S and N shells, respectively. Interestingly, the shell at ∼2.7 Å in the as-isolated sample D cannot be adequately fit by imidazole outer shell scattering. Rather, a heavy atom scatterer (Cu or S) at a distance of ∼2.7 Å appears necessary. This may suggest that some fraction of the copper centers is present in a cluster.

Copper binding data (Table 1) have shown that reduction of hCCS by either dithionite or dithiothreitol reduces the copper binding stoichiometry to 2 coppers per CCS monomer. Therefore, we also investigated the structure of these reduced CCS derivatives by XAS. Figure 2a shows XAS (FTs, EXAFS, and absorption edges) for the dithionite- and DTT-reduced samples, respectively, at a copper concentration of 0.16 mM. Samples of dithionite and DTT-reduced hCCS at a 10-fold higher concentration (sample B, Table 1) gave identical spectra (data not shown). The data for all four samples are essentially identical, indicating that the same species is being formed in each case. However, they differ significantly from the untreated hCCS samples (Figure 1a), and analysis indicates that the N scattering shell has been lost, leaving a S-only environment. Further, the 2.7 Å shell is now well resolved and more intense, and no other outer shells are present. These observations suggest that the reductive dissociation of copper occurs from the histidine-coordinating SOD1-like binding sites in domain II. Thus, the all-S environment of the residual copper sites in the reduced protein likely is derived from the cysteinate residues of domain I and/or domain III.

Curve fitting of the data for the reduced samples produced the fits listed in Table 4. Fits for the 0.16 mM dithionite-reduced sample are shown in Figure 2b (fits to the DTT-reduced samples are essentially identical). The data are well fit to three S at 2.25 ± 0.02 Å and one Cu at 2.72 ± 0.02 Å. The presence of a copper backscatterer at 2.7 Å and the stoichiometry of two coppers bound per CCS monomer are highly suggestive of a dinuclear cluster. The Debye−Waller term for the Cu shell ($2\sigma^2 = 0.009-0.014$ Å^2) suggests a relatively rigid structure and is also consistent with a ligand-bridged cluster (*33*, *37*−*39*). The Cu−S distance is typical of three coordination (*39*) and differs significantly from that found for the bis-cysteinate two-coordinate site of the Menkes protein, which exhibits a Cu−S bond length of 2.17 Å (*18*). Thus, we believe that the simulation data support the presence of a dinuclear cysteine-bridged dicopper(I) cluster in which each copper is coordinated by three cysteine S ligands. Possible structures, consistent with this formulation, are shown in Figure 3. The simulation results for the as-isolated hCCS (Table 3) are easily explained within this framework, since they represent an approximate 1:1 mixture

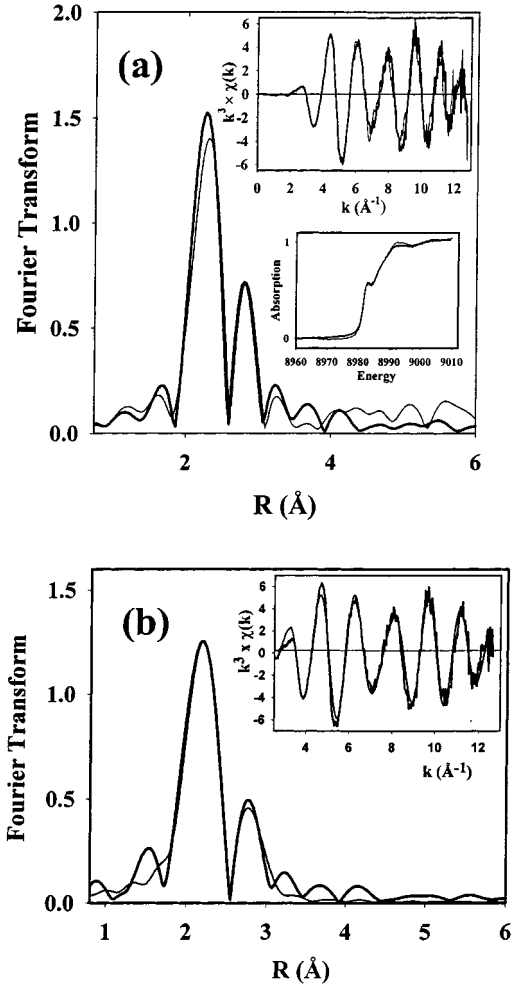

FIGURE 2: Comparison of Fourier transforms, EXAFS (insets to a), and absorption edges (inset to b) for preparations of hCCS reduced with dithiothreitol and sodium dithionite: (a) thin line, sample D [0.16 mM in Cu(I)] + 1.0 mM DTT; thick line, sample D [0.16 mM in Cu(I)] + 1.0 mM dithionite. (b) Experimental (thick lines) versus simulated (thin lines) Fourier transforms and EXAFS (inset) of sample D [0.16 mM in Cu(I)] + 1.0 mM dithionite. Note that the amplitude of the FT peaks is lower than for the spectra shown in panel a due to a shift in k range, which results from applying the theoretical parameter E_0. Parameters used in the fits are given in Table 4.

Table 4: Parameters Used To Simulate the EXAFS Data of the Dithionite- and Dithiothreitol-Reduced Samples of hCCS

		Cu−S[b]			Cu−Cu[b]		
sample	F[a]	shell	R (Å)	$2\sigma^2$ (Å^2)	shell	R (Å)	$2\sigma^2$ (Å^2)
dithionite-reduced 1.6 mM, sample B	0.366	3.0	2.25	0.009	1.0	2.74	0.013
dithionite-reduced 0.16 mM, sample D	0.537	3.0	2.25	0.010	1.0	2.71	0.009
dithiothreitol-reduced 1.1 mM, sample B	0.347	3.0	2.26	0.009	1.0	2.72	0.014
dithiothreitol-reduced 0.16 mM, sample D	0.613	3.0	2.27	0.011	1.0	2.72	0.009
COX17 (ref *38*)		3.0	2.26	0.009	1.0	2.72	0.012

[a] Values of F are influenced by the signal-to-noise ratio of the data sets. Thus they are not necessarily comparable between different samples. [b] Estimated errors in distances are ±0.01 Å for the first shell and ±0.02 Å for outer shells. Estimated errors in coordination numbers are ±25%.

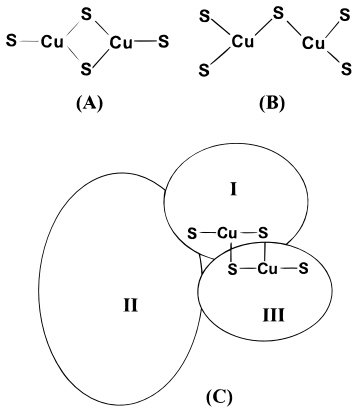

FIGURE 3: Possible structural models for the dinuclear copper cluster in hCCS: (A) double cysteine-bridged cluster with one terminal cysteine per copper; (B) single cysteine-bridged cluster with two terminal cysteine ligands per copper; (C) suggested interaction of domain I and domain III via the dinuclear copper cluster.

of histidine-coordinated SOD1-like binding sites (3 His, 1 Asp) in domain II and the cysteine-bridged dinuclear cluster. It is unclear which of the two potential metal binding sites in domain II are occupied, although both are known to be capable of binding Cu in SOD1 (*30*).

George, Winge, and co-workers (*39*) have reported an essentially identical dinuclear cluster in the cytochrome oxidase chaperone protein COX17. The EXAFS-derived parameters for COX17 are included in Table 4 for comparison to the CCS data. These authors suggested cluster geometries similar to those in Figure 3 but concluded that the doubly bridging μ_2 structure was more consistent with structural data on model complexes. Specifically, the observed Cu−Cu distances in the doubly bridging complexes ranged from 2.7 to 3.0 Å, whereas the Cu−Cu distances in singly bridged clusters were around 3.3 Å. Despite their structural similarities, COX17 and CCS share little sequence homology (*22*, *40*). COX17 is a small (8 kDa) polypeptide, which is likely to exist as a single domain; it contains a CCXC motif and three other conserved cysteines but no MTCXXC motif. The homology of CCS with COX17 thus appears limited to the CXC triad in domain III. hCCS contains six additional Cys residues, three in domain I and three in domain II. In domain I, two cysteines (C22 and C25) reside in the metal binding MTCXXC sequence, while the third (C12) is located close to the N-terminus and is not conserved in yCCS. In domain II, two cysteines are homologous with the SOD1 disulfide cross-link, while the third is likewise not conserved in either yCCS, hSOD1, or ySOD1. Furthermore, tomato CCS contains only four cysteine residues corresponding to the domain I and domain III CXXC and CXC motifs (*41*). Thus, the most likely candidates for copper ligation in hCCS are C22 and C25 in the MTCXXC motif of domain I and C244 and C246 in the CXC motif of domain III.

It is also possible that a dinuclear cluster could form via dimerization of two CCS monomers. Recent evidence suggests that reduced and/or metal-loaded CCS exists primarily as a dimer, with the dimer interface corresponding to the residues in domain II that correspond to the SOD1 dimer interface (*22*, *42*). To investigate this possibility, we collected XAS data on two sets of samples spanning a 10-fold difference in protein concentration (867−75 μM). Both sets of spectra were essentially identical and could be fit with very similar parameters (Table 4). We conclude that intermolecular association is unlikely to be the origin of cluster formation. This conclusion is reinforced by the fact that the putative metal binding sites are at opposite sides of the molecule in the crystallographically characterized dimeric structure and therefore are unlikely to interact. Not unexpectedly, the 2.7 Å shell could also be fit by 1−2 S scatterers at 2.86 Å (minimum in F at 1.2 S, $2\sigma^2 = 0.003$, $F = 0.537$). However, the value of the Debye−Waller term is three times smaller than for the 2.25 Å Cu−S first shell interaction and would be physically unreasonable unless the occupation number of the 2.8 Å Cu−S shell was greater than 1. Since there are two coppers per CCS, any structure based on the fit would require at least four cysteines per copper or eight cysteines per protein, and analysis of the primary sequence data suggests that only four cysteines are candidates for copper ligands in hCCS. Methionine coordination can also be excluded, since it is known that S (Met) scatterers do not contribute strongly to the EXAFS at 2.8 Å (*38*, *43*, *44*). In fact, the dinuclear copper cluster is the only structure which allows both copper ions to be trigonally coordinated by only four cysteine residues.

This conclusion has important structural and function consequences since it implies an interaction between domains I and domain III in hCCS. Truncation mutant studies (*21*) have already demonstrated the importance of domain III in transmetalation and have hinted at a role for domain I in sequestering copper. The finding from XAS that these two domains may bridge via a dinuclear copper cluster in the fully metalated protein suggests that an interdomain protein−protein interaction exists. It is also completely consistent with a recent study of Co^{2+} binding to tomato and human CCS and their domain II/domain III truncation mutants which provided strong evidence for a single Co^{2+} coordinating to all four cysteines of the domain I and domain III metal binding motifs (*41*). This in turn suggests a mechanism for

transfer of a single metal ion from the sequestering site to the translocation site, since the interdomain protein−protein interaction would be expected to form the cluster with one copper site empty. Transfer from domain I to domain III could then take place via a pathway involving a three-coordinate intermediate as previously suggested by Pufahl et al. (*12*).

ACKNOWLEDGMENT

We gratefully acknowledge the use of facilities at the Stanford Synchrotron Radiation Laboratory (SSRL), which is supported by the National Institutes of Health Biomedical Research Technology Program, Division of Research Resources, and by the U.S. Department of Energy, Basic Energy Sciences (BES) and Office of Biological and Environmental Research (OBER).

REFERENCES

1. McCord, J., and Fridovich, I. (1969) *J. Biol. Chem. 244*, 6049−6055.
2. Fridovich, I. (1995) *Annu. Rev. Biochem. 64*, 97−112.
3. Tainer, J. A., Getzoff, E. D., Richardson, J. S., and Richardson, D. C. (1983) *Nature 306*, 284−287.
4. Ogihara, N. L., Parge, H. E., Hart, P. J., Weiss, M. S., Goto, J. J., Crane, B. R., Tsang, J., Slater, K., Roe, J. A., Valentine, J. S., Eisenberg, D., and Tainer, J. A. (1996) *Biochemistry 35*, 2316−2321.
5. Hart, P. J., Balbirnie, M. M., Ogihara, N. L., Nersissian, A. M., Weiss, M. S., Valentine, J. S., and Eisenberg, D. (1999) *Biochemistry 38*, 2167−2178.
6. Rosen, D. R., Siddique, T., Patterson, D., Figlewicz, D. A., Sapp, P., Hentati, A., Donaldson, D., Goto, J., O'Regan, J. P., Deng, H.-X., Rahmani, Z., Krizus, A., McKenna-Yasek, D., Cayabyab, A., Gaston, S. M., Berger, R., Tanzi, R. E., Halperin, J. J., Herzfeldt, B., Van den Bergh, R., Hung, W.-Y., Bird, T., Deng, G., Mulder, D. W., Smyth, C., Laing, N. G., Soriano, E., Pericak-Vance, M. A., Haines, J., Rouleau, G. A., Gusella, J. S., Horvitz, H. R., and Brown, R. H., Jr. (1993) *Nature 362*, 59−62.
7. Deng, H. X., Hentati, A., Tainer, J. A., Iqbal, Z., Cayabyab, A., Hung, W. Y., Getzoff, E. D., Hu, P., Herzfeldt, B., Roos, R. P., Warner, C., Deng, G., Soriano, E., Smyth, C., Parge, H. E., Ahmed, A., Roses, A. D., Hallewell, R. A., Pericak-Vance, M. A., and Siddique, T. (1993) *Science 261*, 1047−1051.
8. Lyons, T. J., Gralla, E. B., and Valentine, J. S. (1999) in *Interrelations Between Free Radicals and Metal Ions in Life Processes* (Sigel, A., and Sigel, H., Eds.) pp 125−177, Marcel Dekker, New York.
9. Lyons, T. J., Liu, H., Goto, J. J., Nersissian, A., Roe, J. A., Graden, J. A., Cafe, C., Ellerby, L. M., Bredesen, D. E., Gralla, E. B., and Valentine, J. S. (1996) *Proc. Natl. Acad. Sci. U.S.A. 93*, 12240−12244.
10. Yim, M. B., Kang, J. H., Yim, H. S., Kwak, H. S., Chock, P. B., and Stadtman, E. R. (1996) *Proc. Natl. Acad. Sci. U.S.A. 93*, 5709−5714.
11. Wiedau-Pazos, M., Goto, J. J., Rabizadeh, S., Gralla, E. B., Roe, J. A., Lee, M. K., Valentine, J. S., and Bredesen, D. E. (1996) *Science 271*, 515−518.
12. Pufahl, R. A., Singer, C. P., Peariso, K. L., Lin, S.-J., Schmidt, P. J., Fahrni, C. J., Cizewski Culotta, V., Penner Hahn, J. E., and O'Halloran, T. V. (1997) *Science 278*, 853−856.
13. Rae, P. J., Schmidt, P. J., Pufahl, R. A., Culotta, V. C., and O'Halloran, T. V. (1999) *Science 284*, 805−808.
14. Culotta, V. C., Klomp, L. W. J., Strain, J., Casareno, R. L. B., Krems, B., and Gitlin, J. (1997) *J. Biol. Chem. 272*, 23469−23472.
15. Casareno, R. L. B., Waggoner, D., and Gitlin, J. D. (1998) *J. Biol. Chem. 273*, 23625−23628.
16. Harrison, M. D., Jones, C. E., and Dameron, C. T. (1999) *J. Biol. Inorg. Chem. 4*, 145−153.
17. Rosenzweig, A. C., Huffman, D. L., Hou, M. Y., Wernimont, A. K., Pufahl, R. A., and O'Halloran, T. V. (1999) *Structure 7*, 605−617.
18. Ralle, M., Cooper, M. J., Lutsenko, S., and Blackburn, N. J. (1998) *J. Am. Chem. Soc. 120*, 13525−13526.
19. Gitschier, J., Moffat, B., Reilly, D., Wood, W. I., and Fairbrother, W. J. (1998) *Nat. Struct. Biol. 5*, 47−54.
20. Steele, R. A., and Opella, S. J. (1997) *Biochemistry 36*, 6885−6895.
21. Schmidt, P. J., Rae, T. D., Pufahl, R. A., Hamma, T., Strain, J., O'Halloran, T. V., and Culotta, V. C. (1999) *J. Biol. Chem. 274*, 23719−23725.
22. Lamb, A. L., Wernimont, A. K., Pufahl, R. A., Culotta, V. C., O'Halloran, T. V., and Rosenzweig, A. C. (1999) *Nat. Struct. Biol. 6*, 724−729.
23. George, G. N. (1990) http://ssrl.slac.stanford.edu/exafspak.html.
24. Ralle, M., Verkovskaya, M. L., Morgan, J. E., Verkovsky, M. I., Wikström, M., and Blackburn, N. J. (1999) *Biochemistry 38*, 7185−7194.
25. Gurman, S. J., Binsted, N., and Ross, I. (1984) *J. Phys. C 17*, 143−151.
26. Gurman, S. J., Binsted, N., and Ross, I. (1986) *J. Phys. C 19*, 1845−1861.
27. Binsted, N., and Hasnain, S. S. (1996) *J. Synchrotron Radiat. 3*, 185−196.
28. Zabinsky, S. I., Rehr, J. J., Ankudinov, A. L., Albers, R. C., and Eller, M. J. (1995) *Phys. Rev. B 52*, 2995−3009.
29. Lamb, A. L., Wernimont, A. K., Pufahl, R. A., O'Halloran, T. V., and Rosenzweig, A. C. (2000) *Biochemistry 39*, 1589−1595.
30. Strothkamp, K. G., and Lippard, S. J. (1982) *Acc. Chem. Res. 15*, 326−332.
31. Garcia-Vasquez, J. A., Romero, J., Castro, R., Sousa, A., Rose, D. J., and Zubieta, J. (1997) *Inorg. Chim. Acta 260*, 221−223.
32. Jannsen, M. D., Spek, A. L., Grove, D. M., and van Koten, G. (1996) *Inorg. Chem. 35*, 4078−4081.
33. Blackburn, N. J., de Vries, S., Barr, M. E., Houser, R. P., Tolman, W. B., Sanders, D., and Fee, J. A. (1997) *J. Am. Chem. Soc. 119*, 6135−6143.
34. Inoue, T., Sugawara, H., Hamanaka, S., Tsukui, H., Suzuki, E., Kohzuma, T., and Kai, Y. (1999) *Biochemistry 38*, 6063−6069.
35. Holm, R. H., Kennepohl, P., and Solomon, E. I. (1996) *Chem. Rev. 96*, 2239−2314.
36. Adman, E. T. (1991) *Adv. Protein Chem. 42*, 145−197.
37. Blackburn, N. J., Barr, M. E., Woodruff, W. H., van der Oost, J., and de Vries, S. (1994) *Biochemistry 33*, 10401−10407.
38. Blackburn, N. J., Ralle, M., Gomez, E., Hill, M. G., Patsuszyn, A., Sanders, D., and Fee, J. A. (1999) *Biochemistry 38*, 7075−7084.
39. Srinivasan, C., Posewitz, M. C., George, G. N., and Winge, D. R. (1998) *Biochemistry 37*, 7572−7577.
40. Glerum, D. M., Shtanko, A., and Tzagoloff, A. (1996) *J. Biol. Chem. 271*, 14504−14509.
41. Zhu, H., Shipp, E., Sanchez, R. J., Liba, A., Stine, J. E., Hart, P. J., Gralla, E. B., Nersissian, A. M., and Valentine, J. S. (2000) *Biochemistry 39*, 5413−5421.
42. Hall, L. T., Sanchez, R. L., Holloway, S. P., Zhu, H., Stine, J. E., Lyons, T. J., Demeler, B., Schirf, V., Hansen, J. C., Nersissian, A. M., Valentine, J. S., and Hart, P. J. (2000) *Biochemistry 39*, 3611−3623.
43. Blackburn, N. J., Rhames, F. C., Ralle, M., and Jaron, S. (2000) *J. Biol. Inorg. Chem.* (in press).
44. Scott, R. A., Hahn, J. E., Doniach, S., Freeman, H. C., and Hodgson, K. O. (1982) *J. Am. Chem. Soc. 104*, 5364−5369.

BI000690J